

Heralded single excitation of atomic ensemble via solid-state-based telecom photon detection

Rikizo Ikuta,¹ Toshiki Kobayashi,¹ Kenichiro Matsuki,¹ Shigehito Miki,² Taro Yamashita,² Hirotaka Terai,² Takashi Yamamoto,¹ Masato Koashi,³ Tetsuya Mukai,⁴ and Nobuyuki Imoto¹

¹*Graduate School of Engineering Science, Osaka University, Toyonaka, Osaka 560-8531, Japan*

²*Advanced ICT Research Institute, National Institute of Information and Communications Technology (NICT), Kobe 651-2492, Japan*

³*Photon Science Center, Graduate School of Engineering,*

The University of Tokyo, Bunkyo-ku, Tokyo 113-8656, Japan

⁴*NTT Basic Research Laboratories, NTT Corporation, Atsugi, Kanagawa 243-0198, Japan*

Telecom photonic quantum networks with matter quantum systems enable a rich variety of applications, such as a long distance quantum cryptography and one-way quantum computing. Preparation of a heralded single excitation (HSE) in an atomic ensemble by detecting a telecom wavelength photon having a correlation with the atomic excitation is an important step. Such a system has been demonstrated with a quantum frequency conversion (QFC) to telecom wavelength employing a Rb atomic cloud. However the limited wavelength selection prevents the next step. Here we for the first time demonstrate HSE with a solid-state-based QFC and a detector for a telecom wavelength that will have a great advantage of the utility of mature telecom technologies. We unambiguously show that the demonstrated HSE indicates a non-classical statistics by the direct measurement of the autocorrelation function.

I. INTRODUCTION

Recent advances in telecom photonic quantum information technology allow integrated photonic circuits, ultra fast switching, and highly efficient single photon detection and wavelength conversion. Combining those technologies with matter quantum systems as shown in Fig. 1 will certainly open up a new avenue for the advanced quantum information technologies, such as a long-distance quantum key distribution [1, 2], quantum computation including measurement-based topological methods [3, 4], and quantum communication among separated nodes [5], and for fundamental tests of the physics outside of the light cone [6]. Manipulation of a quantum state in matter quantum systems has been performed by various wavelengths of the photons [7–12], but the photons in the demonstrations are of visible or near-infrared wavelengths which are not compatible with the telecom regime. Thus to fill the wavelength mismatch, the quantum frequency conversion (QFC) which preserves non-classical photon statistics and a quantum state of an input light has been studied [13].

A pioneering work for this task is a QFC based on a four wave mixing operated around near resonance in cold rubidium (Rb) atoms [14, 15]. In this experiment, a visible photon which heralds spin-wave excitations in cold rubidium (Rb) atoms as a quantum memory was frequency-down-converted to a telecom photon by the QFC by the atomic cloud. The QFC device has a high efficiency due to the operation near atomic resonance. In the meanwhile, it limits choice of wavelengths available to the QFC. Recently widely tunable solid-state-based QFCs have been demonstrated by using various non-linear optical crystals [16–20], and the potential ability for the single photon source with a cold Rb atom ensemble has been demonstrated [21]. However, a heralded single

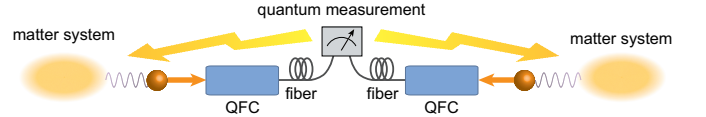


FIG. 1. Concept of an elementary link of quantum matter systems through the optical fiber quantum communication by telecom photons. The telecom photons converted from light pulses which have the correlation with the matter systems are measured for heralding the connection between the quantum matter systems.

excitation (HSE) in long-lived matter quantum system by telecom photon detection required for quantum network illustrated in Fig. 1 has not been demonstrated.

We first show an HSE in a cold Rb atomic ensemble through the detection of the photon emission from D₂ line of Rb. Subsequently, we show the conversion of the wavelength of the photon to 1522 nm in the telecom range by a QFC using a periodically-poled lithium niobate (PPLN) waveguide. Finally we show the demonstration of the HSE through the telecom photon detection by superconducting single photon detectors (SSPDs). Remarkably, we show the non-classical property of the HSE by observing the autocorrelation functions in addition to the cross correlation functions. Furthermore, we show that the telecom photons heralded by the atomic spin state also has a non-classical photon statistics.

II. EXPERIMENTAL SETUP

The ⁸⁷Rb atomic ensemble is prepared by a magneto-optical trap (MOT) for 20 ms. After the lasers and the magnetic field for the MOT are turned off, we use Λ -type

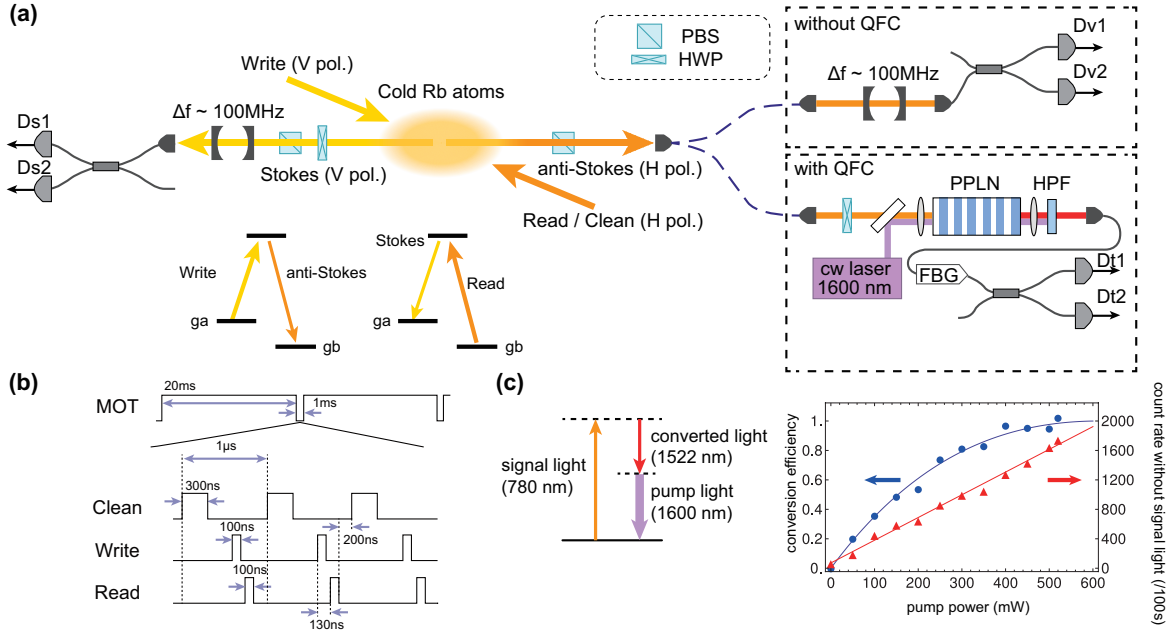


FIG. 2. (a) Our experimental setup without and with the QFC, and the Λ -type energy levels of D_2 line in ^{87}Rb with the relation of the light pulses used in our experiment. The strong write pulse is removed from the optical path of the anti-Stokes photons by the spatial, polarizing and the frequency separation. The filtering of the write pulse from the Stokes photons is performed by the large difference of the spatial direction and the temporal separation. The separation of the read light from the signal photons is performed in the same manner. (b) Time sequence of the experiment. (c) The left figure is the relevant energy levels of QFC. The difference frequency generation of a photon from 780 nm to 1522 nm is performed by using a strong pump light at 1600 nm. The right graph shows the conversion efficiency and the noise counts induced by the frequency converter.

energy levels of D_2 line at 780 nm ($5^2S_{1/2} \leftrightarrow 5^2P_{3/2}$) for the experiment as shown in Fig. 2 (a). Two of the ground levels having $F = 2$ and $F = 1$ are denoted by g_a and g_b , respectively, in which magnetic sublevels are degenerated because of the absence of the magnetic field. At first, a horizontally (H-) polarized 300-ns clean pulse at the resonant frequency between g_b and the excited level ($F' = 2$) prepares the atomic ensemble into g_a . Then a vertically (V-) polarized 100-ns write pulse near the resonant frequency between g_a and the excited level provides the Raman transition from g_a to g_b and anti-Stokes (AS) photons simultaneously. In our experiment, the AS photons emitted in a direction at a small angle ($\sim 3^\circ$) relative to the direction of the write pulse is detected with H polarization. We will explain an optical circuit for the AS photons in detail later. The photon detection in mode AS tells us that the single excitation has been prepared in the atomic ensemble, which we call the heralded single excitation (HSE). In order to read out the HSE, an H-polarized 100-ns read light at the resonant frequency between g_b and the excited level is injected to the atoms. The Raman transition to g_a provides Stokes (S) photons. By setting the direction of the read pulse to be opposite to the write pulse, the Stokes photons are emitted in a mode (S) traveling in the opposite direction to that of mode AS due to the phase matching condition of the four light pulses [22]. In our experiment, we detect

the photons in mode S with V polarization only. The S photons pass through a cavity-based bandpass filter [23] with a bandwidth of ~ 100 MHz, and then they are coupled to a single-mode optical fiber. The photons are divided into two by a fiber-based half beamsplitter (HBS), and then they are detected by silicon avalanche photon detectors (APDs) denoted by D_{s1} and D_{s2} .

Let us explain the optical circuit for the photons in mode AS. The H-polarized AS photons from the atomic ensemble is coupled to a polarization maintaining fiber (PMF). Without QFC, the PMF is connected to an optical circuit for the AS photons passing through a cavity-based bandpass filter with a bandwidth of ~ 100 MHz. After the filtering, the AS photons are divided into two by a HBS. Then they are detected by using APDs denoted by D_{v1} and D_{v2} . With QFC, the PMF is connected to the optical circuit for the QFC. The QFC converts the wavelength of the AS photons from 780 nm to 1522 nm [18, 24]. The conversion efficiency and the background-noise rate induced by the 1600-nm pump light for the conversion with respect to the pump power are shown in Fig. 2 (c). The details of the QFC device are shown in Appendix A.

After the QFC, the 1522-nm photons are coupled to a single-mode optical fiber. The 1522-nm photons pass through a fiber Bragg grating (FBG) with a bandwidth of ~ 1 GHz followed by a HBS. Finally, the 1522-nm pho-

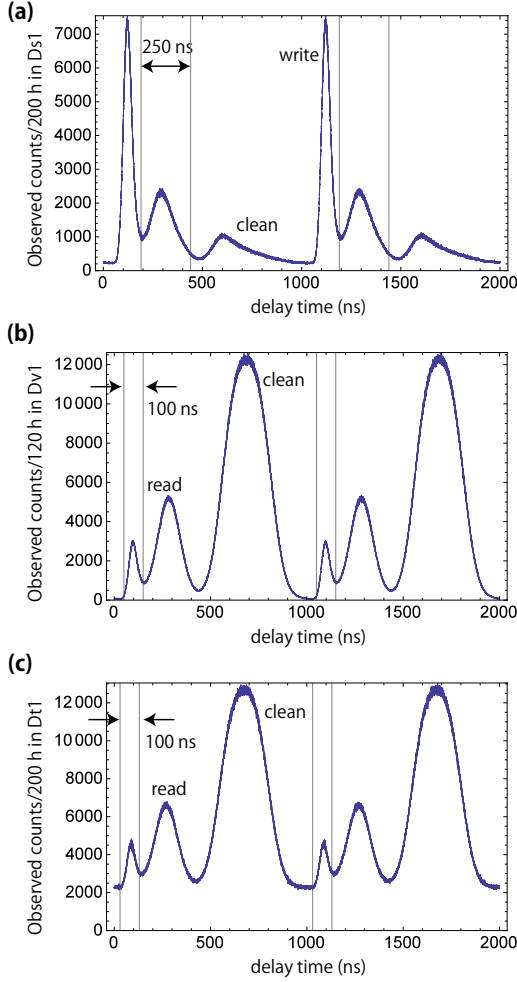


FIG. 3. The observed stop signals by (a) D_{s1} , (b) D_{v1} and (c) D_{t1} . In every figures, the interval of the largest signals is $1 \mu\text{s}$.

tons divided by the HBS are detected by SSPDs [25, 26] denoted by D_{t1} and D_{t2} .

The period of the write pulses is $1 \mu\text{s}$, as shown in Fig. 2 (b). The injection of the write pulses is repeated 990 times until the MOT is turned on again. In each sequence, we collect coincidence events between S and AS photon detections by using a time-digital converter (TDC). A start signal of TDC is synchronized to the timing of triggering the write pulse. All electric signals from photon detections, i.e. D_{s1} , D_{s2} , D_{v1} , D_{v2} , D_{t1} and D_{t2} can be used as stop signals for TDC. Typical histograms of the coincidence events in 1 sequence are shown in Figs. 3 (a)–(c). In the following experiments, we postselect the coincidence events within the 250-ns and 100-ns time windows for the signals of modes S and AS, respectively. In the histograms, while several unwanted peaks coming from the write, read and clean pulses are observed in 1 sequence, they are temporally separated from the main signals and can be eliminated by the selection of the time windows.

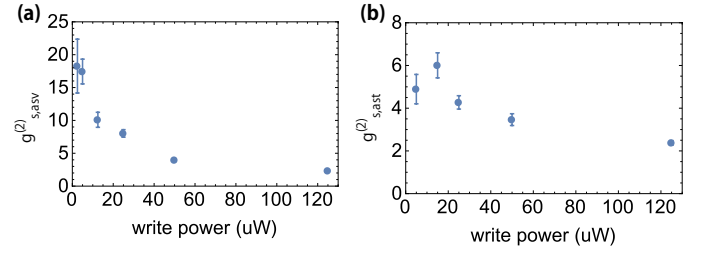


FIG. 4. The dependencies of the cross correlation functions on the power of the write pulse. (a) $g_{s,asv}^{(2)}$ vs write power without the QFC, and (b) $g_{s,ast}^{(2)}$ vs write power with the QFC.

III. EXPERIMENTAL RESULTS

A. Cross correlation function vs. the write power

As a preliminary experiment, we measured the cross correlation function between the Stokes and the anti-Stokes photons with and without QFC for various powers of the write pulse. We denote the detection probabilities of the detectors $D_{s1(2)}$, $D_{v1(2)}$ and $D_{t1(2)}$ by $p_{s1(2)}$, $p_{v1(2)}$ and $p_{t1(2)}$, respectively. We derive the cross correlation functions by the equations $g_{s,asv}^{(2)} = p_{s,v}/(p_s p_v)$ without the QFC and $g_{s,ast}^{(2)} = p_{s,t}/(p_s p_t)$ with the QFC, where p_i is a probability of the photon detection by D_{i1} or D_{i2} for $i = s, v, t$, and $p_{s,v}$ and $p_{s,t}$ are coincidence probabilities between $(D_{s1}$ or $D_{s2})$ & $(D_{v1}$ or $D_{v2})$, and $(D_{s1}$ or $D_{s2})$ & $(D_{t1}$ or $D_{t2})$, respectively. The experimental results are shown in Fig. 4. From Fig. 4 (a), without the QFC, we see that the AS photons which are well correlated with the Stokes photons were prepared for a small power of the write pulse. Fig. 4 (b) shows the cross correlation function when the QFC was performed. We see that the correlation is still kept after the QFC of the AS photons, while its value declines. From the experimental results in Figs. 4 (a) and (b), we set the power of the write pulse to $\sim 15 \mu\text{W}$ in the following experiments.

B. Correlation functions without QFC

Without the QFC, we performed the measurement with an integration measurement time of about 120 hours. The observed cross correlation function was $g_{s,asv}^{(2)} = 9.69 \pm 0.04$. The autocorrelation function $g_{s,s}^{(2)}$ of the photons in mode S without the heralding signal of the photon detection of mode AS was observed by the Hanbury-Brown and Twiss setup [27] using D_{s1} and D_{s2} . It is defined by $g_{s,s}^{(2)} = p_{s1,s2}/(p_{s1} p_{s2})$, where p_{sj} is a probability of the photon detection by D_{sj} for $j = 1, 2$, and $p_{s1,s2}$ is a coincidence probability between D_{s1} and D_{s2} . The observed value was $g_{s,s}^{(2)} = 1.58 \pm 0.03$. Similarly, the autocorrelation function of the AS photons without

| cross correlation functions | | | |
|---|---------------------|-----------------------|-----------------------|
| $g_{s,asv}^{(2)}$ | | $g_{s,ast}^{(2)}$ | |
| 9.69 ± 0.04 | | 4.09 ± 0.01 | |
| autocorrelation functions without heralding signals | | | |
| $g_{s,s}^{(2)}$ | $g_{asv,asv}^{(2)}$ | $g_{ast,ast}^{(2)}$ | |
| 1.58 ± 0.03 | 1.99 ± 0.03 | 1.12 ± 0.01 | |
| autocorrelation functions with heralding signals | | | |
| $g_{s,s asv}^{(2)}$ | $g_{s,s ast}^{(2)}$ | $g_{asv,asv s}^{(2)}$ | $g_{ast,ast s}^{(2)}$ |
| 0.34 ± 0.05 | 0.71 ± 0.10 | 0.47 ± 0.06 | 0.54 ± 0.09 |

TABLE I. The observed values of the correlation functions.

the heralding signal of the photon detection of mode S measured by D_{v1} and D_{v2} was $g_{asv,asv}^{(2)} = 1.99 \pm 0.03$. The autocorrelation function of the S photons heralded by the photon detection of mode AS is denoted by $g_{s,s|asv}^{(2)} = p_{s1,s2,v}p_v/(p_{s1,v}p_{s2,v})$, where $p_{sj,v}$ is a two-fold coincidence probability between D_{sj} and (D_{v1} or D_{v2}) for $j = 1, 2$, and $p_{s1,s2,v}$ is a three-fold coincidence probability among D_{s1} , D_{s2} and (D_{v1} or D_{v2}). The observed autocorrelation function was $g_{s,s|asv}^{(2)} = 0.34 \pm 0.05$. In the case where AS photons heralded by S photons, the autocorrelation function of the heralded AS photons was $g_{asv,asv|s}^{(2)} = 0.47 \pm 0.06$.

C. Correlation functions with QFC

With the QFC, we performed the experiment with an integration time of about 200 hours. The observed cross correlation function between the S and the 1522-nm photons converted from the AS photons was $g_{s,ast}^{(2)} = 4.09 \pm 0.01$. The autocorrelation function of the 1522-nm photons without the heralding signal of the S photons was measured by using D_{t1} and D_{t2} , and the observed value was $g_{ast,ast}^{(2)} = 1.12 \pm 0.01$. The autocorrelation function of the S photons heralded by the 1522-nm photons converted from the AS photons was $g_{s,s|ast}^{(2)} = 0.71 \pm 0.10$. The value remains smaller than 1 after the QFC, and thus we conclude that the demonstrated HSE in Rb atoms shows non-classical statistics with the detection of the 1522-nm photons. In addition, the autocorrelation function of the 1522-nm photons with the heralding signal by the S photons was observed to be $g_{ast,ast|s}^{(2)} = 0.54 \pm 0.09$. In Table I, we list all the observed correlation functions. Especially, autocorrelation functions having less than 1 unambiguously show the non-classical statistics.

From $g_{ast,ast|s}^{(2)} = 0.54$, we can estimate the visibility of Hong-Ou-Mandel (HOM) interference between two independently prepared telecom photons, each of which comes from the atomic ensemble demonstrated here. The visibility of the HOM interference is described by $V = 1/(1 + g_{ast,ast|s}^{(2)})$ with assumptions that mode matching of the signal photons is perfect and stray photons

do not exist (see Appendix B). The estimated value is $V = 0.65$, which exceeds the classical limit of 0.5.

IV. DISCUSSION

In the following, we discuss the degradation of the observed autocorrelation functions with QFC ($g_{s,s|ast}^{(2)}$ and $g_{ast,ast|s}^{(2)}$) with respect to those without QFC ($g_{s,s|asv}^{(2)}$ and $g_{asv,asv|s}^{(2)}$). Because the APDs and the SSPDs have very small dark counts, the observed cross correlation functions and the autocorrelation functions in Table I are considered as intrinsic values of the measured photons. Therefore the degradations from $g_{s,s|asv}^{(2)}$ to $g_{s,s|ast}^{(2)}$ and from $g_{asv,asv|s}^{(2)}$ to $g_{ast,ast|s}^{(2)}$ are mainly caused by the background noise of QFC process of the AS photons. We assume that the background noise is induced by Raman scattering of the QFC pump light which is statistically independent on the signal photons.

Using the definition of the cross correlation functions $g_{s,asv}^{(2)}$ and $g_{s,ast}^{(2)}$, and ratio ζ of the average photon number of the signal in mode AS to the equivalent input noise to the converter, we obtain (see Appendix C)

$$g_{s,ast}^{(2)} = \frac{g_{s,asv}^{(2)}\zeta + 1}{\zeta + 1}. \quad (1)$$

Furthermore $g_{ast,ast}^{(2)}$ is described by

$$g_{ast,ast}^{(2)} = \frac{1}{(1 + \zeta)^2} \left(\zeta^2 g_{asv,asv}^{(2)} + g_{noise}^{(2)} + 2\zeta \right), \quad (2)$$

where $g_{noise}^{(2)}$ is the autocorrelation function of the noise photons [28]. From the observed values ($g_{s,asv}^{(2)}$, $g_{s,ast}^{(2)}$, $g_{asv,asv}^{(2)}$ and $g_{ast,ast}^{(2)}$) and Eqs. (1) and (2), we obtain $\zeta = 0.55$ and $g_{noise}^{(2)} = 0.99$. In Eq. (2), replacing $g_{ast,ast}^{(2)}$, ζ and $g_{asv,asv}^{(2)}$ by $g_{ast,ast|s}^{(2)}$, $\zeta' = g_{s,asv}^{(2)}\zeta$ and $g_{asv,asv|s}^{(2)}$, we have $g_{ast,ast|s}^{(2)} = 0.62$, which is in good agreement with the observed value within the margin of error.

In addition, $g_{s,s|ast}^{(2)}$ is described by using the observed values as (see Appendix C)

$$g_{s,s|ast}^{(2)} = g_{s,s|asv}^{(2)} \left(\frac{g_{s,asv}^{(2)}}{g_{s,ast}^{(2)}} \right)^2 \frac{\zeta}{\zeta + 1} + g_{s,s}^{(2)} \left(\frac{1}{g_{s,ast}^{(2)}} \right)^2 \frac{1}{\zeta + 1}. \quad (3)$$

Thus, from the observed values ($g_{s,s|asv}^{(2)}$, $g_{s,asv}^{(2)}$ and $g_{s,ast}^{(2)}$), and the estimated value of $\zeta = 0.55$, we obtain $g_{s,s|ast}^{(2)} = 0.74$, which is also in good agreement with the experiment.

Below, based on the above estimations, we discuss a possible improvement of $g_{s,s|ast}^{(2)}$ and $g_{ast,ast|s}^{(2)}$ achieved by increasing the value of $\zeta' = g_{s,asv}^{(2)}\zeta$ corresponding to the ratio of the average photon number of the signal in mode AS to the noise induced by QFC conditioned on the photon detection in mode S. For this, we discuss three possible methods without changing the performance of QFC as follows: (a) increase of the collection efficiency of the AS photons, (b) proper selection of the polarization of the AS photons, and (c) refinement of the experimental system for improvement of the correlation functions without QFC. (a) In our experiment, the collection efficiency of the AS photons without QFC is roughly estimated to be several percent (see Appendix D). Here we borrow the collection efficiency of the AS photons from the current state-of-the-art experiments [21, 29], where the value is about ten times larger than that in our experiment, resulting in $\zeta \rightarrow 10\zeta$. This implies that the values of the autocorrelation correlation functions will be $g_{s,s|ast}^{(2)} = 0.39$ and $g_{ast,ast|s}^{(2)} = 0.49$. In this regime, the QFC preserves almost the same statistics as before the conversion shown in Table I. (b) In our experiment, the magnetic sublevels of the ground states g_a and g_b are degenerated, which results in the loss of the AS photons by the polarization selection. Such signal loss is estimated to be about 0.2 under an assumption that the atoms are uniformly distributed in the magnetic sublevels as the initial state (see Appendix E). So its improvement will contribute to increase ζ by a factor of 1.25, resulting in $g_{s,s|ast}^{(2)} = 0.68$ and $g_{ast,ast|s}^{(2)} = 0.60$ from $g_{s,s|ast}^{(2)} = 0.74$ and $g_{ast,ast|s}^{(2)} = 0.62$. (c) Refinement of the measurement for the S photons will increase ζ' through the improvement of $g_{s,asv}^{(2)}$ and other correlation functions without QFC, while ζ is kept. In addition, the use of a smaller excitation probability will also be effective for increasing $g_{s,asv}^{(2)}$ as shown in Fig. 4 (a). While it may need a long time experiment, higher collection probabilities of modes AS and S discussed in (a) may enable us to compensate the reduction of the excitation probability.

V. CONCLUSION

In conclusion, we have clearly shown the HSE in a cold Rb atomic ensemble by detection of the photons at the telecom wavelength, which has been observed by the direct measurement of the autocorrelation function. It was achieved by using the solid-state-based QFC and the detectors with the high efficiency and low noise properties. In addition, we have observed the non-classical photon statistics of the converted telecom photons. It indicates that observation of a non-classical interference between the two telecom photons prepared by duplicating the system demonstrated here will be possible. The quantum system composed of the matter systems and the telecom photons with the solid-state-based QFC and

detectors will be useful for connecting various kinds of matter systems through mature telecom technology.

ACKNOWLEDGEMENTS

This work was supported by MEXT/JSPS KAKENHI Grant Number 26286068, 25247068, 15H03704, 16H02214, 16K17772, and JSPS Grant-in-Aid for JSPS Fellows 14J04677.

Appendix A: Frequency conversion device

The QFC is based on difference frequency generation (DFG) by using a periodically-poled LiNbO₃ (PPLN) waveguide. For the DFG of the signal photon at 780 nm, a V-polarized cw pump laser at 1600 nm with a linewidth of 150 kHz is used. The pump light is combined with the signal photons at a dichroic mirror. Then, they are focused on the type-0 quasi-phase-matched PPLN waveguide. The length of the PPLN crystal is 20 mm, and the acceptable bandwidth is about 0.3 nm which is much wider than that of the signal photons emitted from the atomic ensemble. After passing through the PPLN waveguide, the strong pump light is removed by a high-pass filter and a bandpass filter with a bandwidth of 1 nm. In the measurement of the correlation functions with QFC, we set the pump power to be ~ 200 mW.

Appendix B: Visibility of the HOM interference

Here we consider the HOM interference between two independently prepared signal photons in spatial modes 1 and 2 without any stray photons. The two signal photons are mixed by a HBS, and then the output photons in spatial modes 3 and 4 are detected by detectors D₃ and D₄ with sufficiently wide detection windows. The visibility of the HOM interference is defined by $V = 1 - P_0/P_\infty$. Here P_0 and P_∞ are two-fold coincidence probabilities with $\Delta t = 0$ and $\Delta t = T$, respectively, where T is much larger than the pulse duration of input photons. We assume that when $\Delta t = 0$, mode matching of the input photons is perfect. We also assume that the two input photons have the same values $g_1^{(2)}$ and s_1 of the autocorrelation function and the average photon number, respectively, and are statistically independent. We define that the number operator of spatial mode i ($= 1, 2, 3, 4$) is n_i . By using the normal-ordered product of the operators and bosonic commutation relations, we obtain $P_0/\eta = \langle : n_3 n_4 : \rangle = (\langle : n_1^2 : \rangle + \langle : n_2^2 : \rangle)/4 = s_1^2 g_1^{(2)}/2$, and $P_\infty/\eta = \langle : n_3 n_4 : \rangle = (\langle : n_1^2 : \rangle + \langle : n_2^2 : \rangle + 2\langle : n_1 n_2 : \rangle)/4 = s_1^2 (g_1^{(2)} + 1)/2$, where η is a product of the quantum efficiencies of the detectors. As a result, $V = 1/(1 + g_1^{(2)})$ is obtained.

Appendix C: Derivation of Eqs. (1) and (3)

We derive Eqs. (1) and (3) in the main text. We define that the number operators for mode S, mode AS just before the QFC and the equivalent input noise to the frequency conversion device are n_s , n_{asv} and n_{noise} , respectively. By using the definitions and the normal-ordered product of the operators, we have $\zeta = \langle n_{asv} \rangle / \langle n_{noise} \rangle$, $g_{s,asv}^{(2)} = \langle : n_{asv} n_s : \rangle / (\langle n_s \rangle \langle n_{asv} \rangle)$, $g_{s,s}^{(2)} = \langle : n_s^2 : \rangle / \langle n_s \rangle^2$ and $g_{s,s|asv}^{(2)} = \langle : n_s^2 n_{asv} : \rangle \langle n_{asv} \rangle / (\langle : n_s n_{asv} : \rangle^2)$. Since the noise photons and the S photons are statistically independent, $\langle : n_s n_{noise} : \rangle = \langle n_s \rangle \langle n_{noise} \rangle$ and $\langle : n_s^2 n_{noise} : \rangle = \langle n_s^2 \rangle \langle n_{noise} \rangle$ are satisfied. The number operator n_{ast} for the mode of the 1522-nm photons converted from the AS photons is described by $n_{ast} = \eta_{conv}(n_{asv} + n_{noise})$, where η_{conv} is the efficiency of the QFC. From the relations,

$$\begin{aligned} g_{s,ast}^{(2)} &= \frac{\langle : n_{ast} n_s : \rangle}{\langle n_s \rangle \langle n_{ast} \rangle} \\ &= \frac{g_{s,asv}^{(2)} \zeta + 1}{\zeta + 1} \end{aligned}$$

is derived, which is Eq. (1) in the main text. We also obtain

$$\begin{aligned} g_{s,s|ast}^{(2)} &= \frac{\langle : n_s^2 n_{ast} : \rangle \langle n_{ast} \rangle}{\langle : n_s n_{ast} : \rangle^2} \\ &= \frac{\langle : n_s^2 n_{asv} : \rangle + \langle : n_s^2 : \rangle \langle n_{noise} \rangle}{(g_{s,ast}^{(2)})^2 \langle n_s \rangle^2 (\langle n_{asv} \rangle + \langle n_{noise} \rangle)} \\ &= \frac{g_{s,s|asv}^{(2)} (g_{s,asv}^{(2)})^2 \zeta + g_{s,s}^{(2)}}{(g_{s,ast}^{(2)})^2 (\zeta + 1)} \\ &= g_{s,s|asv}^{(2)} \left(\frac{g_{s,asv}^{(2)}}{g_{s,ast}^{(2)}} \right)^2 \frac{\zeta}{\zeta + 1} + g_{s,s}^{(2)} \left(\frac{1}{g_{s,ast}^{(2)}} \right)^2 \frac{1}{\zeta + 1}, \end{aligned}$$

which is Eq. (3) in the main text.

Appendix D: Estimation of the collection efficiency

We roughly estimate the overall transmittance of the optical circuit of the AS photons. For this, we assume that the photons in modes S and AS generated from the atomic ensemble were initially in the two-mode squeezed state, which does not conflict with the observed values of $g_{s,s}^{(2)} = 1.58 \pm 0.03$ and $g_{asv,asv}^{(2)} = 1.99 \pm 0.03$. We define the overall transmittance of the optical circuit including the collection efficiency of the photons in mode S(AS), the transmittance of the frequency filter and the joint quantum efficiency of $D_{s(v)1}$ and $D_{s(v)2}$ by $\eta_{s(asv)}$. By using the excitation probability p_{ex} , $p_s = p_{ex} \eta_s$, $p_v = p_{ex} \eta_{asv}$ and $p_{s,v} = p_{ex} \eta_s \eta_{asv}$ are satisfied. From the equations and observed counts, we estimated $\eta_{asv} = 0.007$. Assuming that the quantum efficiency 0.6 of the APD and the transmittance 0.25 of the filter, the collection probability of the AS photons is about 0.05. The other parameters

were estimated to be $\eta_s = 0.006$ and $p_{ex} = 0.1$. We similarly estimated the overall transmittance η_{ast} of the circuit for the converted 1522-nm photons detected by $D_{t1(2)}$ to be $\eta_{ast} = 0.003$ which includes the efficiency of the QFC.

Appendix E: Estimation of the loss of the heralded AS photons

We derive the polarization ratio of the AS photons heralded by the V-polarized S photons. For this, we focus on a quantum state of a single atom. By the clean pulse, the atom is initially prepared in g_a ($F = 2$). We denote the atomic state in g_a with magnetic sublevel m_F by $|m_F\rangle$. We first consider a case where the H-polarized AS photons and the V-polarized S photons are detected, which contributes the coincidence detection between modes S and AS in our experiment. Since we use the V-polarized write pulse and the H-polarized read pulse, the transition matrix with respect to the ordered basis $\{|m_F\rangle\}_{m_F=2,\dots,-2}$ from the initial state to the final state in g_a is described by $X_H = X_{2,2'} X_{2',1}^+ X_{1,2}^+ X_{2',2}$, where

$$X_{2',2} = \begin{bmatrix} 0 & \sqrt{\frac{1}{12}} & 0 & 0 & 0 \\ \sqrt{\frac{1}{12}} & 0 & \sqrt{\frac{1}{8}} & 0 & 0 \\ 0 & \sqrt{\frac{1}{8}} & 0 & \sqrt{\frac{1}{8}} & 0 \\ 0 & 0 & \sqrt{\frac{1}{8}} & 0 & \sqrt{\frac{1}{12}} \\ 0 & 0 & 0 & \sqrt{\frac{1}{12}} & 0 \end{bmatrix}, \quad (E1)$$

$$X_{1,2'}^+ = \begin{bmatrix} \sqrt{\frac{1}{4}} & 0 & \sqrt{\frac{1}{24}} & 0 & 0 \\ 0 & \sqrt{\frac{1}{8}} & 0 & \sqrt{\frac{1}{8}} & 0 \\ 0 & 0 & \sqrt{\frac{1}{24}} & 0 & \sqrt{\frac{1}{4}} \end{bmatrix}, \quad (E2)$$

$X_{2',1}^+ = (X_{1,2'}^+)^T$ and $X_{2,2'} = X_{2',2}$, up to a constant factor. The matrix elements are referred from the hyperfine dipole matrix elements for σ^\pm transitions [30]. Next, we consider a case where the V-polarized AS photons and the V-polarized S photons are postselected, which does not contribute the coincidence detection between modes S and AS in our experiment. In this case, the transition matrix with respect to the ordered basis $\{|m_F\rangle\}_{m_F=2,\dots,-2}$ from the initial state to the final state is described by $X_V = X_{2,2'} X_{2',1}^+ X_{1,2}^- X_{2',2}$, where

$$X_{1,2'}^- = \begin{bmatrix} \sqrt{\frac{1}{4}} & 0 & -\sqrt{\frac{1}{24}} & 0 & 0 \\ 0 & \sqrt{\frac{1}{8}} & 0 & -\sqrt{\frac{1}{8}} & 0 \\ 0 & 0 & \sqrt{\frac{1}{24}} & 0 & -\sqrt{\frac{1}{4}} \end{bmatrix}, \quad (E3)$$

under the same constant factor.

We assume that the magnetic sublevel of the initial atomic state in g_a is maximally randomized. In this case,

the ratio of the amount of the H-polarized AS photons to that of the V-polarized AS photons is given by the

ratio of $\text{tr}(X_H^\dagger X_H)$ to $\text{tr}(X_V^\dagger X_V)$. The value is calculated to be 33/8. Thus, in our experimental setup, the loss of the AS photons heralded by the V-polarized S photons is estimated to be $8/41 \sim 0.2$.

-
- [1] A. K. Ekert, “Quantum cryptography based on bells theorem,” *Physical Review Letters* **67**, 661 (1991).
 - [2] H.-K. Lo, M. Curty, and K. Tamaki, “Secure quantum key distribution,” *Nature Photonics* **8**, 595 (2014).
 - [3] T. D. Ladd, F. Jelezko, R. Laflamme, Y. Nakamura, C. Monroe, and J. L. O’Brien, “Quantum computers,” *Nature* **464**, 45 (2010).
 - [4] T. Morimae and K. Fujii, “Blind topological measurement-based quantum computation,” *Nature communications* **3**, 1036 (2012).
 - [5] H. J. Kimble, “The quantum internet,” *Nature* **453**, 1023 (2008).
 - [6] B. Hensen, H. Bernien, A. Dréau, A. Reiserer, N. Kalb, M. Blok, J. Ruitenbergh, R. Vermeulen, R. Schouten, C. Abellán, *et al.*, “Loop-hole-free bell inequality violation using electron spins separated by 1.3 kilometres,” *Nature* **526**, 682 (2015).
 - [7] Z.-S. Yuan, Y.-A. Chen, B. Zhao, S. Chen, J. Schmiedmayer, and J.-W. Pan, “Experimental demonstration of a bdcz quantum repeater node,” *Nature* **454**, 1098 (2008).
 - [8] S. Olmschenk, D. N. Matsukevich, P. Maunz, D. Hayes, L.-M. Duan, and C. Monroe, “Quantum teleportation between distant matter qubits,” *Science* **323**, 486 (2009).
 - [9] S. Ritter, C. Nölleke, C. Hahn, A. Reiserer, A. Neuzner, M. Uphoff, M. Mücke, E. Figueroa, J. Bochmann, and G. Rempe, “An elementary quantum network of single atoms in optical cavities,” *Nature* **484**, 195 (2012).
 - [10] J. Hofmann, M. Krug, N. Ortegel, L. Gérard, M. Weber, W. Rosenfeld, and H. Weinfurter, “Heralded entanglement between widely separated atoms,” *Science* **337**, 72 (2012).
 - [11] H. Bernien, B. Hensen, W. Pfaff, G. Koolstra, M. S. Blok, L. Robledo, T. H. Taminiau, M. Markham, D. J. Twitchen, L. Childress, and R. Hanson, “Heralded entanglement between solid-state qubits separated by three metres,” *Nature* **497**, 86 (2013).
 - [12] A. Delteil, Z. Sun, W.-b. Gao, E. Togan, S. Faelt, and A. Imamoglu, “Generation of heralded entanglement between distant hole spins,” *Nature Physics* **12**, 218 (2015).
 - [13] P. Kumar, “Quantum frequency conversion,” *Optics Letters* **15**, 1476 (1990).
 - [14] A. G. Radnaev, Y. O. Dudin, R. Zhao, H. H. Jen, S. D. Jenkins, A. Kuzmich, and T. A. B. Kennedy, “A quantum memory with telecom-wavelength conversion,” *Nature Physics* **6**, 894 (2010).
 - [15] Y. Dudin, A. Radnaev, R. Zhao, J. Blumoff, T. Kennedy, and a. Kuzmich, “Entanglement of Light-Shift Compensated Atomic Spin Waves with Telecom Light,” *Physical Review Letters* **105**, 260502 (2010).
 - [16] S. Tanzilli, W. Tittel, M. Halder, O. Alibart, P. Baldi, N. Gisin, and H. Zbinden, “A photonic quantum information interface,” *Nature* **437**, 116 (2005).
 - [17] M. T. Rakher, L. Ma, O. Slattey, X. Tang, and K. Srinivasan, “Quantum transduction of telecommunications-band single photons from a quantum dot by frequency up-conversion,” *Nature photonics* **4**, 786 (2010).
 - [18] R. Ikuta, Y. Kusaka, T. Kitano, H. Kato, T. Yamamoto, M. Koashi, and N. Imoto, “Wide-band quantum interface for visible-to-telecommunication wavelength conversion,” *Nature communications* **2**, 1544 (2011).
 - [19] S. Zaske, A. Lenhard, C. Keßler, J. Kettler, C. Hepp, C. Arend, R. Albrecht, W.-M. Schulz, M. Jetter, P. Michler, and C. Becher, “Visible-to-Telecom Quantum Frequency Conversion of Light from a Single Quantum Emitter,” *Physical Review Letters* **109**, 147404 (2012).
 - [20] T. Kobayashi, R. Ikuta, S. Yasui, S. Miki, T. Yamashita, H. Terai, T. Yamamoto, M. Koashi, and N. Imoto, “Frequency-domain hong-ou-mandel interference,” *Nature Photonics* (2016).
 - [21] B. Albrecht, P. Farrera, X. Fernandez-Gonzalvo, M. Cristiani, and H. de Riedmatten, “A waveguide frequency converter connecting rubidium-based quantum memories to the telecom c-band,” *Nature communications* **5**, 3376 (2014).
 - [22] S. Chen, Y.-A. Chen, B. Zhao, Z.-S. Yuan, J. Schmiedmayer, and J.-W. Pan, “Demonstration of a stable atom-photon entanglement source for quantum repeaters,” *Phys. Rev. Lett.* **99**, 180505 (2007).
 - [23] P. Palittapongarnpim, A. MacRae, and A. Lvovsky, “Note: A monolithic filter cavity for experiments in quantum optics,” *Review of Scientific Instruments* **83**, 066101 (2012).
 - [24] R. Ikuta, H. Kato, Y. Kusaka, S. Miki, T. Yamashita, H. Terai, M. Fujiwara, T. Yamamoto, M. Koashi, M. Sasaki, Z. Wang, and N. Imoto, “High-fidelity conversion of photonic quantum information to telecommunication wavelength with superconducting single-photon detectors,” *Physical Review A* **87**, 010301(R) (2013).
 - [25] S. Miki, T. Yamashita, H. Terai, and Z. Wang, “High performance fiber-coupled NbTiN superconducting nanowire single photon detectors with Gifford-McMahon cryocooler,” *Optics Express* **21**, 10208 (2013).
 - [26] T. Yamashita, S. Miki, H. Terai, and Z. Wang, “Low-filling-factor superconducting single photon detector with high system detection efficiency,” *Optics Express* **21**, 27177 (2013).
 - [27] R. Hanbury Brown and R. Q. Twiss, “Correlation between Photons in two Coherent Beams of Light,” *Nature* **177**, 27 (1956).
 - [28] R. Ikuta, T. Kobayashi, S. Yasui, S. Miki, T. Yamashita, H. Terai, M. Fujiwara, T. Yamamoto, M. Koashi, M. Sasaki, *et al.*, “Frequency down-conversion of 637 nm light to the telecommunication band for non-classical light emitted from nv centers in diamond,” *Optics Express* **22**, 11205 (2014).
 - [29] J. Laurat, H. De Riedmatten, D. Felinto, C.-W. Chou, E. W. Schomburg, and H. J. Kimble, “Efficient retrieval of a single excitation stored in an atomic ensemble,” *Optics express* **14**, 6912 (2006).
 - [30] D. A. Steck, “Rubidium 87 D line data,”

(<http://steck.us/alkalidata/> (2001)).